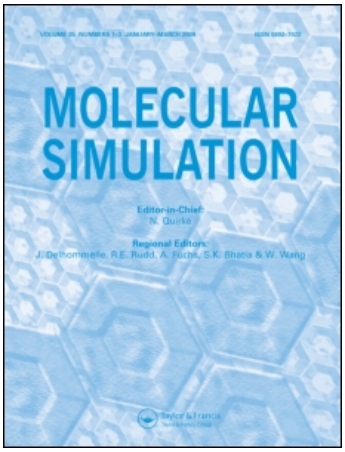

Molecular Simulation
Publication details, including instructions for authors and subscription information:
http://www.informaworld.com/smpp/title~content=t713644482

Molecular dynamics simulations of energy accommodation coefficients for gas flows in nano-channels

Jun Sun[a]; Zhi-Xin Li[a]
[a] Key Laboratory for Thermal Science and Power Engineering of Ministry of Education, School of Aerospace, Tsinghua University, Beijing, P.R. China

To cite this Article Sun, Jun and Li, Zhi-Xin(2009) 'Molecular dynamics simulations of energy accommodation coefficients for gas flows in nano-channels', Molecular Simulation, 35: 3, 228 — 233
To link to this Article: DOI: 10.1080/08927020802395435
URL: http://dx.doi.org/10.1080/08927020802395435

Molecular Simulation
Vol. 35, No. 3, March 2009, 228–233

Taylor & Francis
Taylor & Francis Group

Molecular dynamics simulations of energy accommodation coefficients for gas flows in nano-channels

Jun Sun and Zhi-Xin Li*

Key Laboratory for Thermal Science and Power Engineering of Ministry of Education, School of Aerospace, Tsinghua University, Beijing, P.R. China

(*Received 29 May 2008; final version received 7 August 2008*)

The energy accommodation coefficient (EAC) used in thermal boundary condition in micro- and nano-gas flows is reported to be always less than unity and greatly influenced by wall characteristics, for example, the wall temperature. A statistical EAC definition was described to calculate the EAC for thermal conduction in argon gas between two smooth platinum plates from two-dimensional non-equilibrium molecular dynamics simulations. The non-equilibrium EAC at the upper wall was calculated for different upper wall temperatures and a fixed bottom wall temperature. The equilibrium EAC at each temperature can then be extrapolated from a series of non-equilibrium EACs as the temperature difference between the two walls approaches zero. The analyses of the effects of wall temperature for various Knudsen number on non-equilibrium and equilibrium EACs show that, for a given lower bottom wall temperature, the non-equilibrium EAC at a high temperature wall increases with an increase in the wall temperature. For a given wall temperature difference, the non-equilibrium EAC increases with the increase in the wall temperatures. The equilibrium EAC also becomes larger at higher temperatures.

Keywords: accommodation coefficient; molecular dynamics; micro/nano-scale gas flow

1. Introduction

Micro/nano-electromechanical systems (MEMS/NEMS) have developed rapidly beginning from the 1980s. A great amount of effort has been exerted on the research of MEMS/NEMS devices such as micro-sensors and actuators due to their many potential engineering applications. However, our fundamental understanding of the fluid flow and heat transfer in micro-channels is not able to match the fabrication and utilisation abilities [1,2]. As the channel size decreases to microscale or even smaller sizes, the physics of the micro-gas flows differs from macro-phenomena in at least two key aspects [3]. Firstly, the mean free path (λ) of the gas molecules is comparable to the characteristic length (L, typically the channel height); hence the Knudsen number ($Kn = \lambda/L$) is large enough that rarefaction effects, such as velocity slip and temperature jump on the wall surface, must be considered. Secondly, the surface area to volume ratio is much larger than typical values at macroscale, leading to significant interface effects due to the gas–wall interactions. The relatively large roughness on complicated surfaces and the strong gas–wall interactions will greatly influence the micro-flow and heat transfer. When such size effects are considered, the gas molecules are not always diffusedly reflected by the boundary. The distribution of the reflected gas molecules may be the combination of specular and diffuse reflections described in Maxwell-type boundary conditions.

The energy accommodation coefficient (EAC, also called the thermal accommodation coefficient), first introduced by Maxwell [4] and more clearly defined by Knudsen [5], is an important parameter characterising the microscopic gas–wall interaction processes. EAC is a measure of the average efficiency of the kinetic energy exchange per encounter between gas molecules and wall atoms at the interface [6], and is generally assumed to be unity to express a complete thermal accommodation with the surface in most applications. EAC is used in theoretical analysis of heat transfer in micro-flow to determine the temperature jump at the boundary [7]. A great number of experimental, theoretical and numerical studies [6,8–16] analysing the interactions of gases with metal or semiconductor surfaces to determine accurate values of EAC have shown that it is always less than unity in rarefied gas flows and is influenced by many factors, such as the gas/solid materials, surface roughness and wall temperature. In most studies, the incident gas impinging the surface is a molecular beam or an equilibrium distribution at a temperature different from that of the wall with a Kn large enough to reach the free molecule regime ($Kn > 10$) at very low pressures [11]. However, the conditions are very different in most micro-flows since the incident gas molecules are usually moving randomly and the gas molecules will experience non-equilibrium processes where there are temperature differences between the gas and the surface in the micro-channels. Furthermore, in

*Corresponding author. Email: lizhx@tsinghua.edu.cn

ISSN 0892-7022 print/ISSN 1029-0435 online

DOI: 10.1080/08927020802395435
http://www.informaworld.com

most MEMS/NEMS applications, *Kn* is not extremely large and therefore most micro-gas flows are in the slip flow regime ($0.001 < Kn < 0.1$).

When rarefaction is considered, the continuity assumption is not applicable and the kinetic theory of gases must be used to describe the molecular transport. Many numerical methods based on the Boltzmann equation, such as direct simulation Monte Carlo [17–19] and lattice Boltzmann method [20] can be used to simulate the micro-gas flow well. However, various slip models [6,7,17,20] or other gas–wall interaction models such as the CLL model [21–23] used in these numerical methods still depend on accurate accommodation coefficients (AC) to determine the boundary conditions. The molecular dynamics (MD) method is an efficient and accurate numerical method to determine AC [12–16,25]. In most previous MD simulations [12–16] to calculate AC, the gas molecules near the surface are assumed to interact only with the wall atoms, which may be proper for flows in the free molecular regime. However, in the slip flow regime, gas molecules approaching the wall not only interact with wall atoms but also with other nearby gas molecules. Thus, a new MD algorithm is needed to consider both types of interactions.

To date, there have been few studies of EAC for gas flows and heat transfer in micro/nano-channels. This paper presents an investigation of the EAC of argon (Ar) gas between smooth platinum (Pt) surfaces for microscale thermal conduction using non-equilibrium MD. A statistical algorithm was developed to calculate EAC based on the definition of EAC and to analyse the possible influences of wall temperature and *Kn* on EAC.

2. Numerical methods

2.1 MD method

Molecular dynamics methods have been successfully used to analyse micro/nano-flow in many studies [2,14–16,24–28]. The velocity of the gas molecule is calculated based on Newton's second law using a leap-frog-Verlet algorithm [24] with a time step dt. The computational costs are reduced when using the link-cell method for intermolecular interactions.

The non-equilibrium MD simulation is performed for a two-dimensional system as shown in Figure 1 (similar to that of Cao et al. [25,26]) with a periodic boundary condition in the x-direction in which the length of the computational domain is 0.166 μm. The thermal conduction in the Ar gas is induced by the temperature difference between the two parallel smooth Pt walls at a distance of $H = 0.102$ μm. The walls are built based on the Einstein model theory that the wall atoms are attached to the face-centred-cubic (111) lattice sites by a harmonic spring with a spring constant in both the x- and z-directions

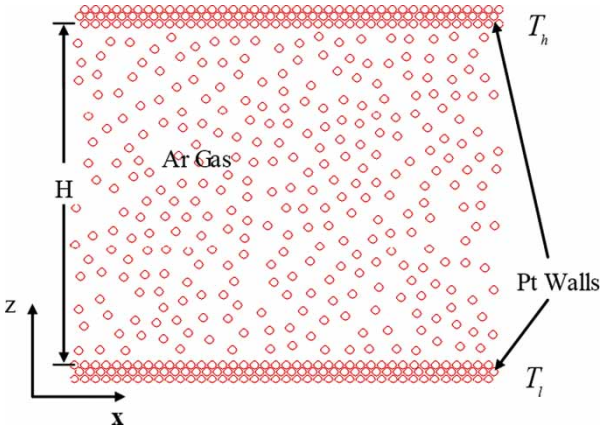

Figure 1. Schematic of computational domain and physical model for MD simulations.

(the angular frequency $\omega = \sqrt{k/m}$ in a spring and $\omega = k_B T_E/\hbar$ in Einstein model, so the spring constant k can be expressed in Equation (1)). While the expression in [24,25] is not right

$$k = \frac{m k_B^2 T_E^2}{\hbar^2}, \tag{1}$$

where m is the mass of the wall atom, k_B the Boltzmann's constant, T_E the Einstein temperature and $\hbar$ is the reduced Planck's constant. For Pt, T_E is 180 K and k equals to 179.5 N/m. In the simulations, the Pt walls are maintained at different constant temperatures by a Langevin thermostat [29] applied in both the x- and z- directions.

A pair of particles (an Ar gas molecule and a Pt atom or a pair of Ar gas molecules) interacts via the Lennard-Jones 6–12 potential:

$$V_{LJ}(r_{ij}) = 4\varepsilon_{ij}\left[\left(\frac{\sigma_{ij}}{r_{ij}}\right)^{12} - \left(\frac{\sigma_{ij}}{r_{ij}}\right)^{6}\right], \tag{2}$$

where r_{ij} is the intermolecular distance for particles i and j, and ε_{ij} and σ_{ij} are the characteristic energy and length parameters. Since this potential vanishes at larger r_{ij}, only the interactions between molecules within a certain cut-off radius, r_c, need be calculated. The parameters for the Lennard-Jones potential and the rest of the simulations are listed in Table 1.

In addition, each case will be simulated repeatedly three times with different initial velocity distributions. In this way, the average statistical results can be calculated with more accuracy.

Table 1. Parameters in the Lennard-Jones potential and other reduced parameters in the simulations [23–25].

Parameter	ε_{Ar-Ar} or ε	σ_{Ar-Ar} or σ	$\tau = \sigma\sqrt{m_{Ar}/\varepsilon}$
Value	1.670×10^{-21} J	3.405×10^{-10} m	2.15×10^{-12} s
Parameter	ε_{Pt-Ar}	σ_{Pt-Ar}	$T_0 = \varepsilon/k_B$
Value	0.894×10^{-21} J	3.085×10^{-10} m	121.0 K

2.2 EAC algorithm

The normal definition of EAC is

$$\alpha = \frac{E_i - E_r}{E_i - E_w}, \tag{3}$$

where E_i and E_r are the average kinetic energies of the gas molecules before and after colliding with the surface and $E_w = (3/2)k_B T_w$ (with streaming correction [6] in two-dimensional conditions) is the average kinetic energy of the reflected molecules in equilibrium with the wall at temperature T_w.

In flows where the incident and reflected gases are in an equilibrium distributions the incident energy E_i and the reflected energy E_r have similar expressions as $E_i = (3/2)k_B T_i$ and $E_r = (3/2)k_B T_r$, where T_i and T_r are the 'effective temperatures' [6] of the incident and reflected gas molecules. Therefore, EAC can be expressed as a function of the wall temperature and the gas temperature:

$$\alpha = \frac{T_i - T_r}{T_i - T_w}, \tag{4}$$

However, the definitions of EAC in Equations (3) and (4) have a potentially serious flaw [6,10] when the denominator becomes zero. The EAC's singularity occurs if the incident energy E_i is equal to E_w or T_i approximates T_w. Thus, the definitions in Equations (3) and (4) are not proper for isothermal flows, but only for flows with a temperature jump near the surface so that the effective temperature of the incident gas differs from the wall temperature resulting in a non-equilibrium EAC. In isothermal flows or where the incident gas is in equilibrium with the wall, EAC is normally referred to as the equilibrium EAC defined as

$$\alpha_E = \lim_{T_i \to T_w} \frac{T_i - T_r}{T_i - T_w}, \tag{5}$$

Thus, the equilibrium EAC is a function of T_w as the incident gas temperature approaches the wall temperature.

From Equation (3), the calculation of the non-equilibrium EAC must distinguish between the incident and the reflected molecules in each time step during the computational process. The short-range forces between molecules mean that a gas molecule far from the wall interact only with the other gas molecules. When the gas molecule moves closer to the wall, the gas–wall interactions will gradually become important. The molecular velocity normal to the wall may reverse due to the strong gas–wall interactions in only one time step, or at most several time steps, after which the molecule bounces away from the wall and the gas–wall interactions weaken. This is referred to as the incidence–reflection process shown in Figure 2. In MD simulations, the time at which the gas molecule approaching the wall starts to interact with the wall atoms is called the incident time, while the time at which the gas–wall force on the molecules leaving the wall approaching zero is referred to as the reflected time. By distinguishing between the incident and the reflected molecules, the non-equilibrium EAC calculated from Equation (3) will converge to a time-averaged stable value over a large number of time steps. Generally speaking, for $dt = 0.005\tau$, 5 million time steps are required for the system to reach a steady state, with another 15 million time steps necessary to calculate the non-equilibrium EAC and other statistical data.

The equilibrium EAC cannot be acquired directly in the same way due to the singularity in isothermal flows. As shown in Equation (5), the equilibrium EAC is the limit of a series of non-equilibrium EACs as the gas temperature approaches the wall temperature. Therefore, a reasonable method, which has also been implemented experimentally [6], is to estimate the equilibrium EAC at each temperature from a series of non-equilibrium EACs with various temperature differences between the gas and the wall.

2.3 Selection of cut-off radius in simulations

The cut-off radius as an important computational parameter in the above-mentioned algorithm can affect the accuracy and divergence of the predicted statistical non-equilibrium EAC.

The cut-off radius, r_c, in the Lennard-Jones potential has a significant effect on the motion of the incident and

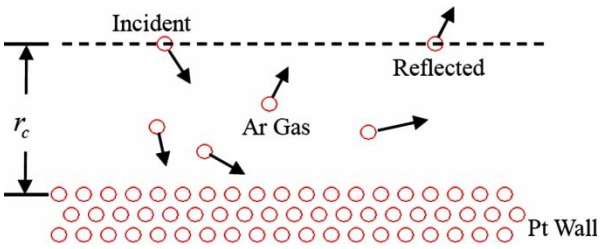

Figure 2. Schematic of the algorithm for determining the incident and reflected gas molecules.

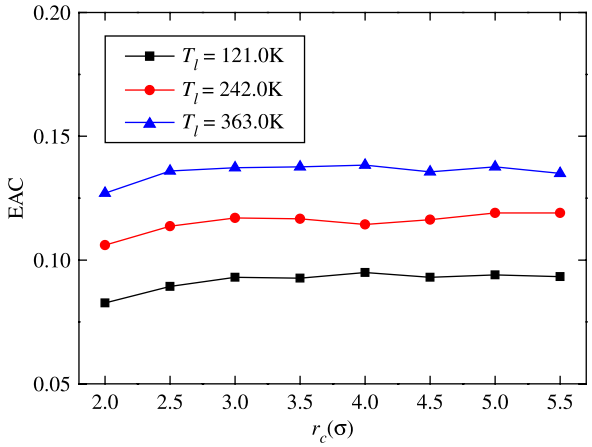

Figure 3. Non-equilibrium EAC for various cut-off radii, r_c, and various bottom wall temperatures, T_l, for $Kn = 0.1726$ and $T_h - T_l = 242.0$ K.

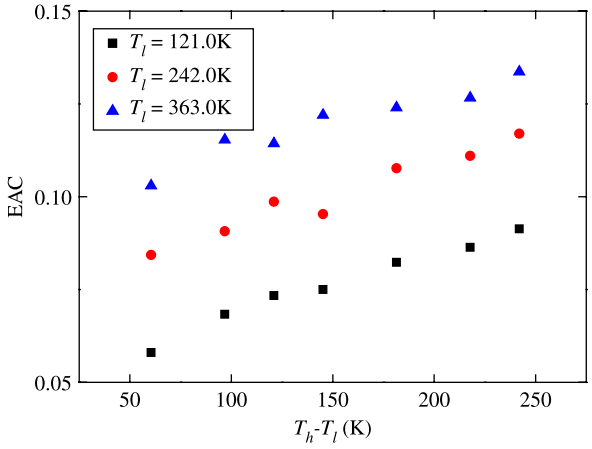

Figure 4. Non-equilibrium EAC for various wall temperature differences, $T_h - T_l$, and various bottom wall temperatures, T_l, for $Kn = 0.0575$.

the reflected gas molecules, and, consequently, the non-equilibrium EAC calculations. Therefore, several r_c ranging from 2.0σ to 5.5σ were employed to evaluate the effect of the cut-off radius on the non-equilibrium EAC value. The bottom wall temperatures were maintained at T_0, $2T_0$ and $3T_0$, where $T_0 = 121.0$ K is indicated in Table 1.

The non-equilibrium EAC for high-temperature walls is shown in Figure 3 for the same wall temperature difference of $T_h - T_l = 242.0$ K and 1000 Ar gas molecules ($Kn = 0.1726$, Kn values are calculated using two-dimensional hard sphere model in [26]) in the simulation system. The largest standard deviation in this part is less than 0.010. In each case group, the non-equilibrium EAC for $r_c \geq 3.0\sigma$ is lower than the others, while for $r_c \geq 3.0\sigma$, the non-equilibrium EAC is similar with very small fluctuations around a stable value due to statistical errors. Therefore, in all the following simulations, r_c is taken as 3.0σ to reduce the computational costs.

3. Results and discussion

According to Equation (4), the non-equilibrium EAC is a function of the gas temperature and the wall temperature. In the simulations, the temperature influence on the non-equilibrium EAC was analysed by varying the wall temperatures. Changes in the upper and bottom wall temperatures will change the gas temperature distribution in the system and the gas temperature near the wall, and consequently influence the non-equilibrium EAC.

The non-equilibrium EAC for $Kn = 0.0575$ (with 3000 gas molecules in the system) is shown in Figure 4 with the bottom temperatures fixed at 121.0, 242.0 and 363.0 K, respectively, for the wall temperature differences ranging from 60.5 to 242.0 K. The largest standard deviation in these cases is less than 0.012. Figure 4 indicates that the non-equilibrium EAC increases with the increase in the wall temperature for a given wall temperature difference, which means that non-equilibrium EAC is a function of wall temperature. Figure 4 also shows that the non-equilibrium EAC increases with the increase in the wall temperature difference (increased the upper wall temperature) for a fixed bottom wall temperature, which means that it is also affected by the wall temperature difference. In summary, both the wall temperature and the wall temperature difference affect the non-equilibrium EAC. The larger the wall temperature difference is and the higher the wall temperature is, the larger the non-equilibrium EAC will be.

Table 2. Non-equilibrium EAC for $T_l = 242.0$ K with various Kn.

Non-equilibrium EAC	$Kn = 0.1726$	$Kn = 0.0863$	$Kn = 0.0575$
$T_h - T_l = 60.5$ K	0.083 ± 0.008	0.080 ± 0.010	0.084 ± 0.011
$T_h - T_l = 96.8$ K	0.092 ± 0.010	0.099 ± 0.015	0.091 ± 0.010
$T_h - T_l = 121.0$ K	0.096 ± 0.008	0.099 ± 0.009	0.099 ± 0.009
$T_h - T_l = 145.2$ K	0.100 ± 0.009	0.105 ± 0.011	0.095 ± 0.007
$T_h - T_l = 181.5$ K	0.104 ± 0.007	0.106 ± 0.011	0.108 ± 0.005
$T_h - T_l = 217.8$ K	0.111 ± 0.008	0.110 ± 0.004	0.111 ± 0.003
$T_h - T_l = 242.0$ K	0.115 ± 0.007	0.118 ± 0.010	0.117 ± 0.001

Furthermore, *Kn* can be changed by changing the number of gas molecules in the simulation system. The non-equilibrium EAC results for $T_l = 242.0$ K are listed in Table 2 for three different *Kn* values. For a fixed bottom and upper wall temperatures, the non-equilibrium EAC for different *Kn* values is almost the same considering computational errors. Thus, the effect of *Kn* on the non-equilibrium EAC is not explicit.

Yamamoto [14] and Yamamoto et al. [15] also calculated the non-equilibrium EAC for Ar gas and Pt wall interactions in a micro-thermal conduction problem using MD method coupled with DSMC method. The impinging gas molecules were considered to interact only with the wall and the Morse potential values with larger ε_{Ar-Pt} (about 1.859×10^{-21} J, twice of that in this paper) were used for the gas–wall interactions. Since a stronger gas–wall interaction potential will lead to more accommodation with the wall, the non-equilibrium EAC for smooth walls in [14] (0.43) and [15] (0.41–0.49) is larger than the data in our simulations (all less than 0.2). Therefore, the interaction potential and the related parameters in MD simulation should be paid more attention to.

As noted in the previous part, the equilibrium EAC for isothermal flows cannot be calculated directly by analysing the kinetic energies of the incident and reflected gas molecules as with the non-equilibrium EAC. Therefore, the equilibrium EAC is predicted from a series of non-equilibrium EACs for upper wall temperatures close to the bottom wall temperature. As T_h approaches T_l, the equilibrium EAC at T_l can be extrapolated linearly from the non-equilibrium EAC in Figure 4. The predicted equilibrium EACs are listed in Table 3 and illustrated in Figure 5 as a function of temperature for various *Kn* values. For the same *Kn* value, the equilibrium EAC decreases as the temperature increases. While at the same temperature, the equilibrium EACs do not change much for different *Kn* values.

4. Conclusions

Non-equilibrium MD simulations of thermal conduction in Ar gas between smooth Pt walls were used to investigate the effects of wall temperature (121.0–605.0 K) for various values of *Kn* (0.0575–0.1726) on the non-equilibrium and equilibrium EACs. A new algorithm was developed to predict the non-equilibrium EAC, and consequently the equilibrium EAC extrapolated from a series of non-equilibrium EACs.

Table 3. Predicted equilibrium EAC for various temperatures and *Kn*.

Equilibrium EAC	$Kn = 0.1726$	$Kn = 0.0863$	$Kn = 0.0575$
$T = 121.0$ K	0.059	0.058	0.050
$T = 242.0$ K	0.075	0.077	0.074
$T = 363.0$ K	0.099	0.089	0.098

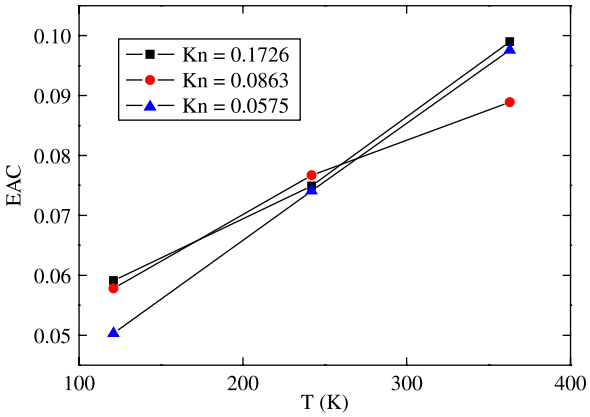

Figure 5. Equilibrium EAC for various temperatures and various *Kn*.

All the predicted EAC in these simulations are much less than unity. The simulations indicate that the non-equilibrium and equilibrium EACs are both sensitive to the temperature. For a fixed bottom wall temperature, the non-equilibrium EAC at the upper wall increases with the increasing upper wall temperature and the increasing wall temperature difference. With a fixed temperature difference between the two walls, the non-equilibrium EAC is larger for larger wall temperatures. The predicted equilibrium EAC also increases with increasing temperature.

In addition, different interaction models and the effect of a stronger gas–wall interaction on EAC should be considered in the future work.

Acknowledgements

The authors thank Dr M.R. Wang and Dr B.Y. Cao for their helpful discussions. This computational work has been supported by Tsinghua National Laboratory for Information Science and Technology, P.R. China.

References

[1] C.M. Ho and Y.C. Tai, *Micro-electro-mechanical-systems (MEMS) and fluid flows*, Annu. Rev. Fluid Mech. 30 (1998), pp. 579–612.
[2] M. Gad-el-Hak, *Gas and liquid transport at the microscale*, Heat Transfer Eng. 27(4) (2006), pp. 13–29.
[3] Z.Y. Guo and Z.X. Li, *Size effect on microscale single-phase flow and heat transfer*, Int. J. Heat Mass Transfer 46 (2003), pp. 149–159.
[4] J.C. Maxwell, *On stresses in rarified gases arising from inequalities of temperature*, Philos. Trans. R. Soc. Lond. 170 (1879), pp. 231–256.
[5] M. Knudsen, *The Kinetic Theory of Gases: Some Modern Aspects*, Methuen, London, 1934.
[6] F.O. Goodman and H.Y. Wachman, *Dynamics of Gas–Surface Scattering*, Academic Press, New York, 1976.

[7] A. Beskok, *Simulations and Models for Gas Flows in Micro-geomitries*, Ph.D. diss., MIT, Cambridge, 1996.
[8] C.T. Rettner and M.N.R. Ashfold, *Dynamics of Gas–Surface Interactions*, Royal Society of Chemistry, London, 1991.
[9] C.T. Rettner, *Thermal and tangential momentum accomodation coefficients for N_2 colliding with surfaces of relevance to disk-drive air bearings derived from molecular beam scattering*, IEEE Trans. Magn. 34(4) (1998), pp. 2387–2395.
[10] J.C. Tully, *Dynamics of gas-surface interaction: 3D generalized Langevin model applied to fcc and bcc surfaces*, J. Chem. Phys. 73(4) (1980), pp. 1975–1985.
[11] H. Ambaye and J.R. Manson, *Calculations of accomodation coefficients for diatomic molecular gases*, Phys. Rev. E. 73 (2006), 031202.
[12] V. Chirita, B.A. Pailthorpe, and R.E. Collins, *Non-equilibrium energy and momentum accomodation coefficients of Ar atoms scattered from Ni (001) in the thermal regime: a molecular dynamics study*, Nuclear Instrum. Methods Phys. Res. B. 129 (1997), pp. 465–473.
[13] J. Blomer and A.E. Beylich, *Molecular dynamics simulation of energy accomodation of internal and translational degrees of freedom at gas–surface interfaces*, Surface Sci. 423(1) (1999), pp. 127–133.
[14] K. Yamamoto, *Slip flow over a smooth platinum surface*, JSME Int. J. Ser. B Fluids Therm. Eng. 45(4) (2002), pp. 788–795.
[15] K. Yamamoto, H. Takeuchi, and T. Hyakutake, *Effect of wall characteristics on the behaviours of reflected gas molecules in a thermal problem*, in *Rarefied Gas Dynamics*, A.D. Ketsdever and E.P. Muntz, eds., AIP, New York, 2003, pp. 1008–1015.
[16] K. Yamamoto, H. Takeuchi, and T. Hyakutake, *Characteristics of reflected gas molecules at a solid surface*, Phys. Fluids. 18(4) (2006), 046103.
[17] G.A. Bird, *Molecular Gas Dynamics and the Direct Simulation of Gas Flows*, Oxford University Press, New York, 1994.
[18] M.R. Wang and Z.X. Li, *Simulations for gas flows in microgeometries using the direct simulation Monte Carlo method*, Int. J. Heat Fluid Flow 25(6) (2004), pp. 975–985.
[19] M.R. Wang and Z.X. Li, *An Enskog based Monte Carlo method for high Knudsen number non-ideal gasflows*, Comput Fluids 36(8) (2007), pp. 1291–1297.
[20] S. Chen and G. Doolen, *Lattice Boltzmann method for fluid flows*, Annu. Rev. Fluid Mech. 30 (1998), pp. 329–364.
[21] C. Cercignani and M. Lampis, *Kinetic models for gas-surface interactions*, Transp. Theory Stat. Phys. 1(2) (1971), pp. 101–114.
[22] R.G. Lord, *Application of C-L-scattering kernal to DSMC calculation*, in *Rarefied Gas Dynamics*, A.E. Beylich, ed., VCH, Weinheim, 1991, pp. 1427–1433.
[23] R.G. Lord, *Some extensions to the C-L gas-surface scattering kernal*, Phys. Fluids. A 3(4) (1991), pp. 706–710.
[24] M.P. Allen and D.J. Tildesley, *Computer Simulation of Liquids*, Oxford University, New York, 1989.
[25] B.Y. Cao, M. Chen, and Z.Y. Guo, *Temperature dependence of the tangential momentum accomodation coefficient for gases*, Appl. Phys. Lett. 86 (2005), 091905.
[26] B.Y. Cao, M. Chen, and Z.Y. Guo, *Application of 2DMD to gaseous microflows*, Chin. Sci. Bull. 49 (2004), pp. 1101–1105.
[27] M.R. Wang, J. Liu, and S. Chen, *Similarity of electro-osmotic flows in nanochannels*, Mol. Simul. 33(3) (2007), pp. 239–244.
[28] M.R. Wang, J. Liu, and S. Chen, *Electric potential distribution in nanoscale electroosmosis: from molecules to continuum*, Mol. Simul. 33(15) (2007), pp. 1273–1277.
[29] G.S. Grest and K. Kremer, *Molecular dynamics simulation of polymers in the presence of a heat bath*, Phys. Rev. A. 33(5) (1986), pp. 3628–3631.